the resulting error estimates are dominated by the width of the features used and become larger (in absolute terms) as the features become older. The crests of M1 and M2 are 10 m and 50 m wide, respectively, at their widest in the field and on the satellite images.
15. Sampling was performed in September 2001. Samples were typically well-embedded blocks of vein quartz ~20 cm in diameter or, occasionally, chips removed from exposed parts of larger samples. Beryllium extraction procedures and production rate calculations follow those described by Mériaux *et al*. (*5, 30*). The ratios of cosmogenic ^{10}Be to stable isotope ^{9}Be were determined by accelerator mass spectrometry at the Lawrence Livermore National Laboratory Center for Accelerator Mass Spectrometry.
16. J. Imbrie *et al.*, in *Milankovitch and Climate, Part I*, A. Berger, J. Imbrie, J. Hays, G. Kukla, B. Saltzman, Eds. (Reidel, Boston, 1984), pp. 269–305.
17. R. C. Finkel, L. A. Owen, P. L. Barnard, M. W. Caffee, *Geology* **31**, 561 (2003).
18. L. A. Owen *et al.*, *Geol. Soc. Am. Bull.* **115**, 1356 (2003).
19. C. Lasserre, G. Peltzer, F. Crampe, *Eos* **42**, F271 (2001).
20. P. Segall, *Int. Geol. Rev.* **44**, 62 (2002).
21. J. C. Savage, W. H. Prescott, *J. Geophys. Res.* **83**, 3369 (1978).
22. H. Perfettini, J. P. Avouac, *J. Geophys. Res.* **109**, art. no. B06402 (2004).
23. G. Peltzer, F. Crampe, S. Hensley, P. Rosen, *Geology* **29**, 975 (2001).
24. A. Hubert-Ferrari *et al.*, *Geophys. J. Int.* **153**, 111 (2003).
25. R. Bendick, R. Bilham, J. Freymueller, K. Larson, G. H. Yin, *Nature* **404**, 69 (2000).
26. K. Wallace, G. H. Yin, R. Bilham, *Geophys. Res. Lett.* **31**, art. no. L09613 (2004).
27. A. Mériaux *et al.*, *J. Geophys. Res.*, in press.
28. R. Weldon, K. Scharer, T. Fumal, G. Biasi, *GSA Today* **14**, 4 (2004).
29. R. A. Bennett, A. M. Friedrich, K. P. Furlong, *Geology* **32**, 961 (2004).
30. Materials and methods are available as supporting material on *Science* Online.
31. This work was performed under the auspices of the U.S. Department of Energy by University of California Lawrence Livermore National Laboratory under contract W-7405-Eng-48 under the sponsorship of the Laboratory Directed Research and Development program (report no. UCRL-JRNL-206541). Also supported by the Institut National des Sciences de l'Univers, Centre National de la Recherche Scientifique (Paris, France), through programs Imagerie et Dynamique de la Lithosphère and Intérieur de la Terre, and by the China Earthquake Administration and the Ministry of Lands and Resources (Beijing, China).

Supporting Online Material
www.sciencemag.org/cgi/content/full/307/5708/411/DC1
Materials and Methods
Figs. S1 to S5
Tables S1 to S2
References and Notes

21 September 2004; accepted 15 December 2004
10.1126/science.1105466

Speciation by Distance in a Ring Species

Darren E. Irwin,[1]* Staffan Bensch,[2] Jessica H. Irwin,[1] Trevor D. Price[3]

Ring species, which consist of two reproductively isolated forms connected by a chain of intergrading populations, have often been described as examples of speciation despite gene flow between populations, but this has never been demonstrated. We used amplified fragment length polymorphism (AFLP) markers to study gene flow in greenish warblers (*Phylloscopus trochiloides*). These genetic markers show distinct differences between two reproductively isolated forms but gradual change through the ring connecting these forms. These findings provide the strongest evidence yet for "speciation by force of distance" in the face of ongoing gene flow.

Traditional models emphasize geographic separation as a necessary prerequisite to speciation (*1*, *2*). Although experiments and theory indicate that species can form despite ongoing gene flow (*3–5*), there are very few known examples in nature (*2*). Some studies have demonstrated divergence despite gene flow (*6*, *7*), but they do not enable an assessment of reproductive isolation because the divergent forms remain geographically separated. Species are usually defined as groups of interbreeding populations reproductively isolated from other such groups (*1*, *2*), and this can only be critically examined if different populations regularly come into contact in nature.

There are a few examples where reproductively isolated populations coexist while being connected by apparently gradual variation around geographic barriers ["ring species"; reviewed in (*8*)]. In theory, ring species enable us to trace the process by which one species diverges into two. They also potentially show that reproductive isolation can arise in the face of gene flow (*1*, *8–10*). However, a clear pattern of a gradual genetic variation has not previously been observed in a ring species. Here, we use molecular markers to show that two reproductively isolated forms of greenish warbler (*Phylloscopus trochiloides*) are connected by gene flow through a ring of populations, providing the strongest empirical evidence yet for "speciation by force of distance" (*1*, *9*).

Two forms of greenish warbler, one in west Siberia (*P. t. viridanus*) and one in east Siberia (*P. t. plumbeitarsus*; Fig. 1), coexist without interbreeding in central Siberia and can therefore be considered separate species (*10*). These forms are connected by a chain of populations to the south that encircles the high-altitude desert of the Tibetan Plateau, which is not inhabited by the warblers. Through this chain of populations, traits such as color patterns, morphology, and behaviors (song and song recognition), change gradually, demonstrating a smooth gradient in forms between two species (*10*, *11*). There is evidence that all of these traits are under selection in the *Phylloscopus* warblers (*10–15*); it is therefore unclear that such traits can be used to infer gene flow. To directly measure genome-wide genetic relationships, we used amplified fragment length polymorphism (AFLP) markers (*16*).

From 105 greenish warblers at 26 sites throughout the breeding range we obtained 62 AFLP markers that were variable and could be scored unambiguously as present or absent in each individual (*17*). West Siberian *viridanus* and east Siberian *plumbeitarsus* are clearly separated in AFLP genotypes, which confirms that the two taxa are genetically distinct. In contrast, AFLP genotypes change gradually through the ring of populations to the south (Fig. 1). The genetic gradient in the AFLP genotypes around the southern ring of populations is best seen in a plot of pairwise AFLP distances versus pairwise geographic distance (Fig. 2). Geographic distances were measured under the assumption that no genes flow across the uninhabited area in the center of the ring or between *viridanus* and *plumbeitarsus* in central Siberia. Thus, "corrected" distances between west Siberian (*viridanus*) and east Siberian (*plumbeitarsus*) populations were measured through the long chain of populations running to the south of Tibet, through the Himalayas. Genetic distance and corrected geographic distance are strongly correlated (Mantel's $r = 0.782$, $P = 0.0003$), consistent with a pattern of isolation by distance (*18*) around the ring. An alternative analysis based on pairwise F_{ST} distances between populations produces similar results (Mantel's $r = 0.677$, $P = 0.0012$; table S1 and fig. S3).

On the basis of these results, we conclude that there is no break in gene flow through the ring of populations, except between the divergent forms *viridanus* and *plumbeitarsus* in central Siberia. Thus all populations have been recently connected by at least some gene

[1]Department of Zoology, University of British Columbia, 6270 University Boulevard, Vancouver, BC, Canada V6T 1Z4. [2]Department of Animal Ecology, Lund University, S-223 62 Lund, Sweden. [3]Department of Ecology and Evolution, University of Chicago, 1101 E. 57th Street, Chicago, IL 60637, USA.

*To whom correspondence should be addressed. E-mail: irwin@zoology.ubc.ca

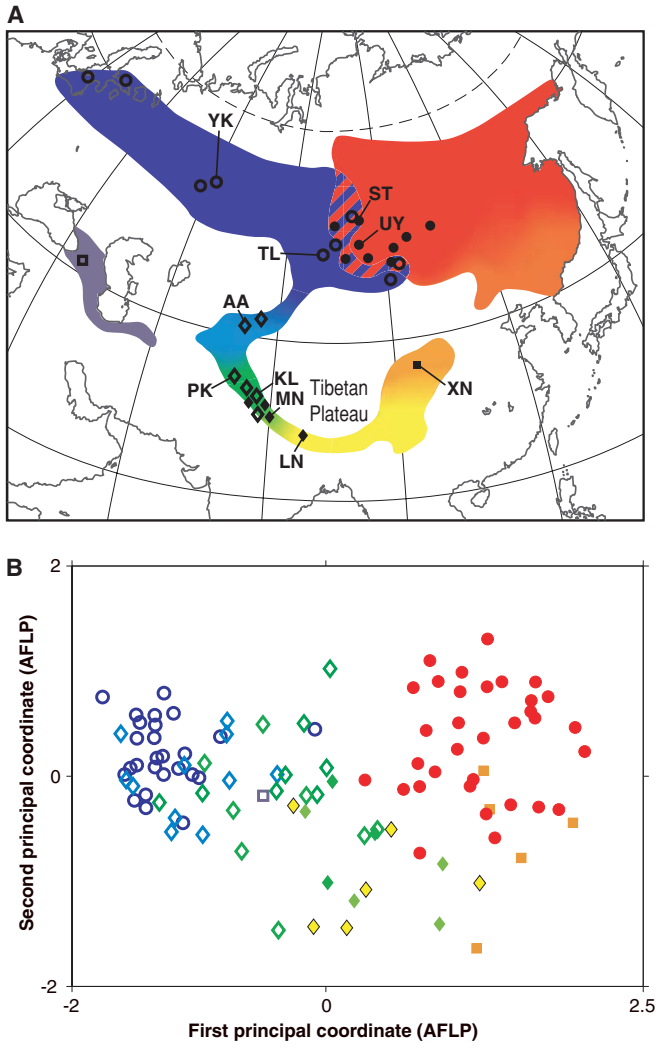

Fig. 1. (A) Map of Asia showing the range of greenish warblers in the breeding season. Different colors represent different subspecies as designated by Ticehurst (*20*) (*P. t. viridanus*, blue; *ludlowi*, green; *trochiloides*, yellow; *obscuratus*, orange; *plumbeitarsus*, red; and *nitidus*, violet). Colors grade together in areas where Ticehurst described gradual morphological change. The hatched area in central Siberia indicates the overlap zone between *viridanus* and *plumbeitarsus*. The gap in the ring in northern China is likely due to recent habitat destruction (*10*). Sampling sites are indicated by symbols corresponding to major mitochondrial clades [open symbols indicate western clade, and closed symbols eastern, see fig. S1 and (*10*)], with the most important sites indicated by two-letter codes. (B) Geographic variation in 62 AFLP markers as summarized by principal coordinates analysis. Each symbol represents a single individual, and distance between symbols corresponds roughly to genetic distance. Colors and symbols correspond to (A). Although the northern subspecies *viridanus* and *plumbeitarsus* differ distinctly in their genetic characteristics, there is gradual genetic change through the southern chain of populations. PC1 explains 19.4% of the variance, PC2 5.6%.

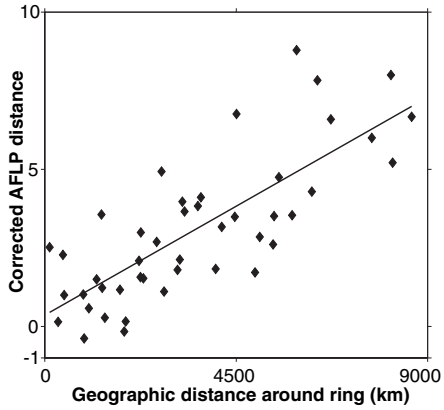

Fig. 2. Genetic distance based on AFLP markers increases with geographic distance measured around the southern ring (that is, if one assumes no direct gene flow between *viridanus* and *plumbeitarsus* or across the uninhabited area in the center of the ring). Corrected average pairwise distances between populations were calculated as the mean number of pairwise differences between two populations minus the average distance between individuals within those populations. For purposes of illustration, a least-squares regression line is fit to all points.

flow. The simplest historical scenario for this result is that short-distance dispersal in a continuously distributed species has resulted in a pattern of isolation by distance (*18*).

This interpretation may at first seem inconsistent with previously published patterns of variation in mitochondrial DNA (mtDNA) (*10*) (fig. S1), in which there are several deep phylogeographic breaks around the ring, the deepest of which is in the western Himalayas. In fact, the mtDNA and AFLP patterns are compatible. Short-distance dispersal in a continuously distributed species is expected to cause phylogeographic structuring in mtDNA clades (*19*) and a pattern of isolation by distance in AFLP markers (*18*). The shape of the greenish warbler range is particularly suited to creating this pattern; the birds breed in a narrow string of treeline habitat through the Himalayas, where dispersal distances are likely shorter than in more broadly distributed forest habitat further north. Ticehurst (*20*) hypothesized that the greenish warblers were at one time confined to the Himalayas and then expanded northward along two pathways into Siberia. Theory predicts that the pattern of isolation by distance should be weaker in regions of recent range expansion compared with regions that have been inhabited over a long period of time (*18*). The steeper genetic change seen in AFLPs (figs. S2 and S3), mtDNA, and two microsatellite loci (*10*) through the Himalayas than through regions to the north is consistent with this prediction. It is also possible that these patterns were influenced by temporary breaks in gene flow due to geographic barriers in the Himalayas; however, such barriers, if they existed, did not cause reproductive isolation to evolve in that region.

Greenish warblers provide the only known example of a smooth genetic gradient between two genetically differentiated and reproductively isolated forms, providing rare insight into how speciation can occur. Patterns of variation in ecologically and sexually selected traits of greenish warblers suggest that latitudinal gradients in environmental characteristics, such as forest density and seasonal migration distance, during the two northward expansions into Siberia have resulted in rapid evolutionary adaptation, divergence, and reproductive isolation (*8*, *10*, *11*).

Several authors (*4*, *21*) have suggested on theoretical grounds that ring species or "sexual continua" are unstable and will fairly quickly break into two or more species that do not exchange genes. The two models that show this effect do not apply well to the greenish warbler, because one (*4*) does not include local adaptation throughout a continuous geographic range and the other (*21*) does not include different geographic locations for different populations. We suggest that ring species such as the greenish warbler, in which local adaptation occurs along a long and nearly continuous ring of populations, could be stable indefinitely. This stability could be interrupted by processes such as habitat change, which could increase the likelihood of parapatric speciation (*5*), or habitat destruction, which could divide the continuous range and thereby increase the likelihood of additional species boundaries forming.

References and Notes

1. E. Mayr, *Systematics and the Origin of Species* (Dover Publications, New York, 1942).
2. J. A. Coyne, H. A. Orr, *Speciation* (Sinauer Associates, Sunderland, MA, 2004).
3. W. R. Rice, E. E. Hostert, *Evolution* **47**, 1637 (1993).
4. S. Gavrilets, H. Li, M. D. Vose, *Proc. R. Soc. London B Biol. Sci.* **265**, 1483 (1998).
5. M. Doebeli, U. Dieckmann, *Nature* **421**, 259 (2003).
6. T. B. Smith, R. K. Wayne, D. J. Girman, M. W. Bruford, *Science* **276**, 1855 (1997).

7. C. J. Schneider, T. B. Smith, B. Larison, C. Moritz, *Proc. Natl. Acad. Sci. U.S.A.* **96**, 13869 (1999).
8. D. E. Irwin, J. H. Irwin, T. D. Price, *Genetica* **112-113**, 223 (2001).
9. T. Dobzhansky, in *A Century of Darwin*, S. A. Barnett, Ed. (Heinemann, London, 1958), pp. 19–55.
10. D. E. Irwin, S. Bensch, T. D. Price, *Nature* **409**, 333 (2001).
11. D. E. Irwin, *Evolution* **54**, 998 (2000).
12. A. D. Richman, T. Price, *Nature* **355**, 817 (1992).
13. K. Marchetti, *Nature* **362**, 149 (1993).
14. A. V. Badyaev, E. S. Leaf, *Auk* **114**, 40 (1997).
15. K. Marchetti, T. Price, *Oikos* **79**, 410 (1997).
16. U. G. Mueller, L. L. Wolfenbarger, *Trends Ecol. Evol.* **14**, 389 (1999).
17. Materials and methods are available as supporting material on *Science* Online.
18. M. Slatkin, *Evolution* **47**, 264 (1993).
19. D. E. Irwin, *Evolution* **56**, 2383 (2002).
20. C. B. Ticehurst, *A Systematic Review of the Genus* Phylloscopus (Johnson Reprint Corp., New York, 1938).
21. A. J. Noest, *Proc. R. Soc. London B. Biol. Sci.* **264**, 1389 (1997).

22. Supported by an International Research Fellowship grant from the National Science Foundation (to D.E.I.) and the Swedish Research Council (to S.B.) plus grants for fieldwork by the National Geographic Society and National Science Foundation (to T.D.P.). We thank Z. Benowitz-Fredericks, J. Gibson, S. Gross, G. Kelberg, A. Knorre, K. Marchetti, and B. Sheldon for assistance in the field, and P. Alström, K. Marchetti, U. Olsson, A. Richman, J. Tiainen, and the Burke Museum for additional samples. R. Calsbeek, M. Whitlock, and several anonymous reviewers provided helpful comments.

Supporting Online Material

www.sciencemag.org/cgi/content/full/307/5708/414/DC1
Materials and Methods
Figs. S1 to S3
Table S1
References

14 September 2004; accepted 17 November 2004
10.1126/science.1105201

Large Sulfur Bacteria and the Formation of Phosphorite

Heide N. Schulz[1]* and Horst D. Schulz[2]

Phosphorite deposits in marine sediments are a long-term sink for an essential nutrient, phosphorus. Here we show that apatite abundance in sediments on the Namibian shelf correlates with the abundance and activity of the giant sulfur bacterium *Thiomargarita namibiensis*, which suggests that sulfur bacteria drive phosphogenesis. Sediments populated by *Thiomargarita* showed sharp peaks of pore water phosphate (≤300 micromolar) and massive phosphorite accumulations (≥50 grams of phosphorus per kilogram). Laboratory experiments revealed that under anoxic conditions, *Thiomargarita* released enough phosphate to account for the precipitation of hydroxyapatite observed in the environment.

The formation of phosphorites in marine sediments is a major long-term sink for phosphorus, removing it from the biosphere. The initial step in phosphorite formation is the precipitation of phosphate-containing minerals, for example, hydroxyapatite, followed by many other processes such as sediment transport, winnowing, and re-crystallization (*1*, *2*). A fundamental problem in explaining massive phosphorite deposits has been identifying mechanisms that can concentrate pore water phosphate enough to drive spontaneous precipitation of phosphorus minerals. Here we suggest a new mechanism, the episodic release of phosphate into the anoxic sediment by an abundant benthic bacterium that is specially adapted to survive under both oxic and anoxic conditions. *Thiomargarita* periodically contacts oxic bottom water in order to take up nitrate, and it survives long intervals of anoxia with nitrate stored internally (*3*). The phosphate uptake from different sources occurs when *Thiomargarita* forms thick mats at the sediment surface or is suspended in the oxic water column.

The giant sulfur bacterium *Thiomargarita namibiensis* occurs in high biomass in surface sediments off the coast of Namibia (*3*). Like its close relatives *Beggiatoa* spp. and *Thioploca* spp., this bacterium gains energy by oxidizing sulfide, which accumulates in anoxic marine sediments as a result of the degradation of organic matter by sulfate-reducing bacteria. The production of sulfide is directly proportional to the amount of organic carbon in the sediment, thus these large sulfide-oxidizing bacteria are abundant in highly productive upwelling areas, where the flux of organic material to the sea floor is high. *Thiomargarita* and *Beggiatoa* dominate sediments beneath the Benguela upwelling area off Namibia (*3*), whereas *Thioploca* dominates sediments off the South American west coast (*4*) and in the Arabian Sea (*5*). In all of these areas, modern phosphorite formation has been reported (*1*, *6*). All of these sulfur bacteria species contain large amounts of intracellular polyphosphates, which we found by staining cells specifically for polyphosphate with toluidine blue (*7*, *8*). Also, these bacteria show electron-dense inclusions (*3*, *9*, *10*), which is a typical appearance of polyphosphate.

During an expedition with the German research vessel *Meteor* off the coast of Namibia in March 2003, we found high pore water phosphate concentrations (*7*) of up to 300 μM in sediments that were densely populated by *T. namibiensis* (Fig. 1A). The sharp phosphate peaks that were observed in sediments were restricted to a narrow sediment horizon (about 3 cm thick), which corresponded to the depths where *T. namibiensis* was most abundant (Fig. 1C). Because of the high phosphate concentrations, active formation of phosphorite occurred in this thin zone as indicated by the large amounts of phosphorus-containing minerals in the sediment (*7*) (>50 g kg^{-1} of dry sediment or 5% P) (Fig. 1B). The predominant phosphorus mineral phase was hydroxyapatite [$Ca_5OH(PO_4)_3$], which was determined by x-ray diffraction (XRD) analysis (*7*). Fifty grams of P per kg of sediment is equivalent to 270 g of hydroxyapatite per kg of sediment. Therefore, more than 25% of the solid phase in this layer was hydroxyapatite, which is one of the major

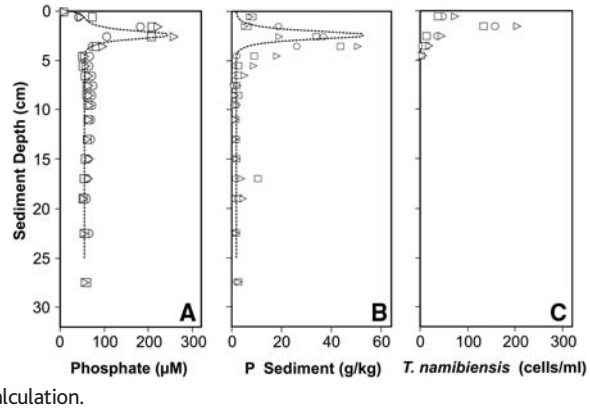

Fig. 1. Sediment profiles from the Namibian shelf (22°10′S, 14°03′E; water depth 70 m). (**A**) Phosphate concentrations in the pore water (μM) at different sediment depths (cm). (**B**) Phosphorus content of dried sediment (g kg^{-1}) at different sediment depths. (**C**) Biomass of *T. namibiensis* (cells ml^{-1}) at different sediment depths. Three parallel measurements are shown as indicated by the different symbols. The dashed lines show the steady-state concentration of pore water phosphate and the amount of phosphorus accumulating as predicted by the model calculation.

[1]Institute for Microbiology, University of Hannover, Schneiderberg 50, D-30167 Hannover, Germany. [2]Department of Geosciences, University of Bremen, Klagenfurter Strasse, D-28359 Bremen, Germany.

*To whom correspondence should be addressed. E-mail: schulz@ifmb.uni-hannover.de

SUPPORTING ONLINE MATERIAL

Speciation by Distance in a Ring Species

Darren E. Irwin, Staffan Bensch, Jessica H. Irwin, and Trevor D. Price

Materials and methods

Previously, we examined variation in mitochondrial DNA sequences (~1200 bp from the neighborhood of the control region and ND6 gene) from 149 greenish warblers from 27 sites throughout their breeding range (*S1*). Here we summarize those data in a haplotype network calculated by the program TCS (*S2*) and drawn by hand (Fig. S1). In this study we used the same samples for AFLP analysis. Because AFLP requires DNA extracts of a higher concentration and quality than simple PCR amplification of mtDNA requires, only 105 of the samples (from 26 sites) were suitable for AFLP genotyping.

We used the protocol of Bensch et al. (*S3*), which was based on the method of Vos et al. (*S4*). We used the restriction enzymes *Eco*RI and *Tru*I to digest genomic DNA, and then synthetic oligonucleotides ("adaptors") were ligated to the fragments. Next, we performed two rounds of PCR using primers corresponding to, in the first round, the adaptor plus 1 arbitrary base pair, and in the second round, the adaptor plus 3 arbitrary base pairs. Flourescein-labelled primers were used in the second round of PCR (the "selective amplification"). The products were separated in 6% denaturing polyacrylamide gels and visualized using a Vistra FluorImager.

We obtained 62 AFLP markers that were variable and could be scored unambiguously, from three primer combinations (19 markers with $E_{TCT}xM_{CGA}$, 23 with $E_{TGA}xM_{CGT}$, 20 with $E_{TAG}xM_{CAT}$). AFLP bands were scored as absence/presence data. Each of the 105 individuals in the analysis had a unique multilocus genotype. We summarized variation in the resulting 0/1 matrix by performing a principal coordinate analysis (PCO) using the R package (*S5*). Given a matrix of pairwise genetic distances among individuals, this procedure determines the major axes of variation in the data set. We present results (Fig. 1B) based on Euclidean distances, but similar results were obtained with other distance measures, such as squared Euclidean distances and Jaccard distances. We used the program Arlequin (*S6*) to calculate corrected average pairwise distances between populations (the mean number of pairwise differences between two populations minus the average distance between individuals within those populations). Arlequin was also used to calculate pairwise F_{ST} values between populations. Note that this method of calculating F_{ST} makes no assumption regarding Hardy-Weinberg equilibrium.

To test for a pattern of isolation by distance, we performed a Mantel test using the R Package (*S5*) to compare corrected AFLP distances between populations with geographic distances through the ring of greenish warbler populations. These "corrected" geographic distances were measured assuming a barrier to gene flow spanning from central Siberia south into the Tibetan Plateau. Thus corrected distances between west Siberian (*viridanus*) and east Siberian (*plumbeitarsus*) populations were measured through the long chain of populations running to the south of Tibet. To determine a single axis representing geographic location around the ring (e.g. in Fig. S2), we performed a principal coordinates analysis on the matrix of corrected geographic distances. The first principal coordinate axis explained 57% of the variation in the corrected geographic distances, and this was then used as a measure of geographic location around the ring.

Fig. S1. Mitochondrial DNA haplotype network showing six major clades and the divergence between them, based on data described in (*S1*). Colors correspond to the location where each haplotype was sampled according to Fig. 1, and the area of each circle is proportional to the number of samples with that haplotype. Missing haplotypes are indicated by black dots. The symbols next to each clade indicate the symbol used on the map (Fig. 1a) that corresponds to that clade. There are two major mitochondrial clades that overlap both in central Siberia, where they delineate reproductively isolated forms (*S1*), and within the subspecies *ludlowi* in the western Himalayas, where they do not correspond to reproductively isolated forms.

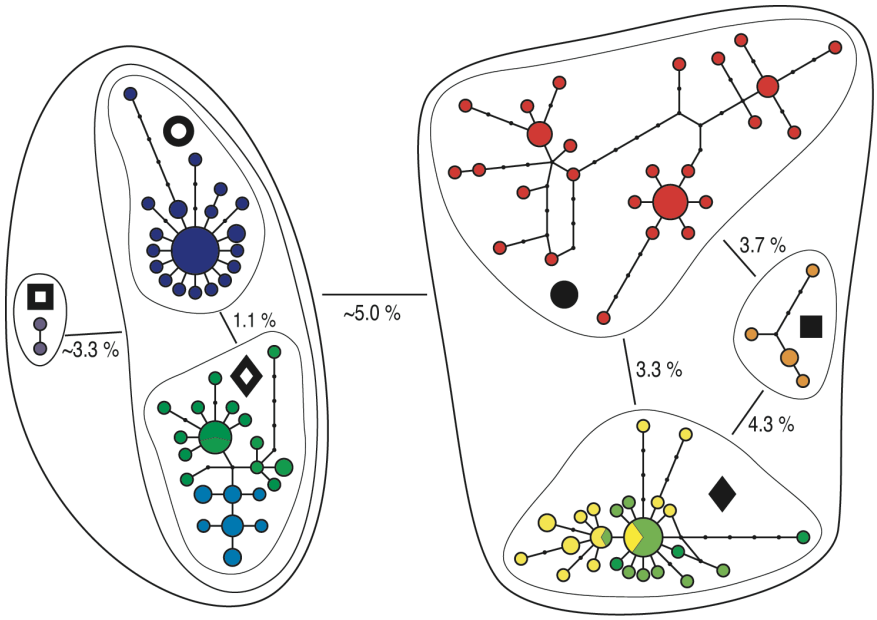

Supplemental results

Comparison of mtDNA and AFLP. **Fig. S2.** Patterns of variation around the southern side of the ring, measured from west Siberia (on left) around the southern side of Tibet to east Siberia (on right) for mitochondrial haplotypes (top) and AFLP genotypes (bottom). Each vertical axis corresponds to the first principal coordinate axis, with a principal coordinate analysis conducted for the mtDNA distances in a similar way as the AFLP distances. Each point represents a single individual, and the different symbols indicate different mitochondrial clades according to Figs. 1 and S1. See the Methods above for a description of how location was determined for this figure. The much sharper discontinuities in the mtDNA are expected for a single non-recombining molecule (*S7*).

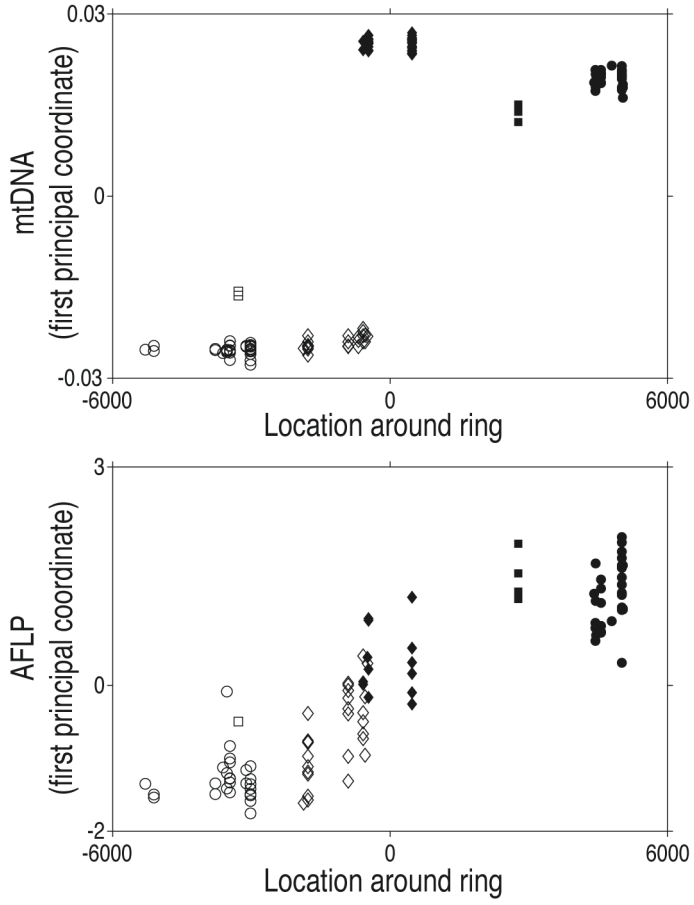

Analysis based on Fst values. **Fig. S3.** Diagram showing geographic relationships of major sampling sites and pairwise F_{ST} values between geographically close sites based on AFLP variation. Symbols correspond to different mtDNA clades (Fig. S1). The F_{ST} values through the southern chain of populations are much less than those between west Siberian *viridanus* and east Siberian *plumbeitarsus*.

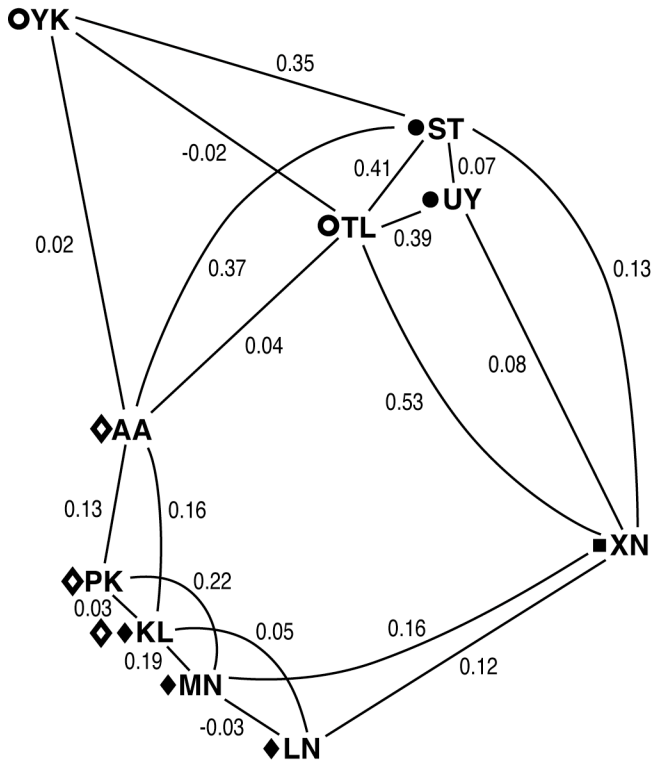

Table S1. Pairwise measures of divergence between major sampling sites.

	YK	TL	AA	PK	KL	MN	LN	XN	ST	UY
YK	7.73	7.04	7.60	10.33	11.05	14.50	13.17	17.00	17.36	15.78
TL	-0.02	6.68	7.20	10.16	11.41	14.94	13.58	17.43	18.16	16.04
AA	0.02	0.04	7.16	10.03	10.46	13.80	12.70	15.64	16.99	14.57
PK	**0.11**	**0.16**	**0.13**	10.43	10.93	14.81	13.00	14.80	16.00	15.04
KL	**0.16**	**0.24**	**0.16**	0.03	10.76	14.57	12.10	14.34	16.95	14.93
MN	**0.30**	**0.38**	**0.32**	**0.22**	**0.19**	13.33	12.42	14.10	17.00	15.08
LN	**0.24**	**0.32**	**0.26**	**0.13**	0.05	-0.03	12.27	13.00	16.44	14.67
XN	**0.47**	**0.53**	**0.46**	**0.29**	**0.26**	0.16	0.12	10.60	14.21	13.17
ST	**0.35**	**0.41**	**0.37**	**0.24**	**0.27**	**0.20**	**0.21**	**0.13**	13.64	14.52
UY	**0.33**	**0.39**	**0.33**	**0.22**	**0.19**	0.11	0.13	0.08	0.07	13.40

Above the diagonal are average AFLP distances between populations. On the diagonal are average AFLP distances within populations. Below the diagonal are F_{ST} between populations. Bold F_{ST} values are significant at the $P<0.005$ level.

References – Online Supplement

S1. D. E. Irwin, S. Bensch, T. D. Price, *Nature* **409**, 333 (2001).

S2. M. Clement, D. Posada, K. A. Crandall, *Mol. Ecol.* **9**, 1657 (2000).

S3. S. Bensch, A. J. Helbig, M. Salomon, I. Seibold, *Mol. Ecol.* **11**, 473 (2002).

S4. P. Vos *et al.*, *Nucleic Acids Research* **23**, 4407 (1995).

S5. P. Casgrain, P. Legendre. *The R Package for Multidimensional and Spatial Analysis* (<http://www.fas.umontreal.ca/biol/casgrain/en/labo/R/> Département de sciences biologiques, Université de Montréal, 2001).

S6. S. Schneider, D. Roessli, L. Excoffier. *Arlequin: A Software for Population Genetics Data Analysis. Ver 2.000.* (<http://lgb.unige.ch/arlequin/> Genetics and Biometry Laboratory, University of Geneva, Switzerland, 2000).

S7. D. E. Irwin, *Evolution* **56**, 2383 (2002).